Ribosomal protein L35 is required for 27SB pre-rRNA processing in *Saccharomyces cerevisiae*

Reyes Babiano and Jesús de la Cruz*

Departamento de Genética, Universidad de Sevilla, Sevilla, Spain

ABSTRACT

Ribosome synthesis involves the concomitance of pre-rRNA processing and ribosomal protein assembly. In eukaryotes, this is a complex process that requires the participation of specific sequences and structures within the pre-rRNAs, at least 200 *trans*-acting factors and the ribosomal proteins. There is little information on the function of individual 60S ribosomal proteins in ribosome synthesis. Herein, we have analysed the contribution of ribosomal protein L35 in ribosome biogenesis. *In vivo* depletion of L35 results in a deficit in 60S ribosomal subunits and the appearance of half-mer polysomes. Pulse-chase, northern hybridization and primer extension analyses show that processing of the 27SB to 7S pre-rRNAs is strongly delayed upon L35 depletion. Most likely as a consequence of this, release of pre-60S ribosomal particles from the nucleolus to the nucleoplasm is also blocked. Deletion of *RPL35A* leads to similar although less pronounced phenotypes. Moreover, we show that L35 assembles in the nucleolus and binds to early pre-60S ribosomal particles. Finally, flow cytometry analysis indicated that L35-depleted cells mildly delay the G1 phase of the cell cycle. We conclude that L35 assembly is a prerequisite for the efficient cleavage of the internal transcribed spacer 2 at site C_2.

INTRODUCTION

Ribosomes are highly complex ubiquitous ribonucleoparticles that are responsible for translating the mRNA into proteins (1). In all cells, ribosomes are composed of two ribosomal subunits (r-subunits). Recently, the structural complexity of the eubacterial and archaeal ribosomes has been obtained at the atomic resolution (2). Molecular models of eukaryotic ribosomes have also been documented for yeast and mammals. Although the resolution of these models is much lower than that from the crystals, its analysis reveals that eukaryotic ribosomes are more complex but display considerable structural similarity to their prokaryotic counterparts (3,4).

Ribosome biogenesis is a complicated pathway that requires the coordinated assembly of the ribosomal RNAs (16S, 5S and 23S rRNAs in prokaryotes, 18S, 5S, 5.8S and 25S rRNAs in eukaryotes) with the r-proteins (about 50 different proteins in prokaryotes and about 80 in eukaryotes) to yield the two r-subunits. In eukaryotes, this takes place largely within the nucleolus (5,6) although late steps occur in the nucleoplasm and even in the cytoplasm (5,7,8). Ribosome biogenesis is evolutionary conserved throughout eukaryotes (9) but it has been studied most extensively in the yeast *Saccharomyces cerevisiae* (10,11). In the yeast nucleolus, a large precursor rRNA (pre-rRNA) encoding the mature 18S, 5.8S and 25S rRNAs is synthesized by RNA polymerase I whereas a pre-5S is independently transcribed by RNA polymerase III (12). The pre-rRNA processing pathway is now almost fully known and requires a series of sequential endo- and exonucleolytic reactions that are mediated by endo- and exonucleases (for details, see Supplementary Figure S1). Pre-rRNA maturation (processing and rRNA modification) and the assembly of pre-rRNA with r-proteins occur concomitantly, and the overall process requires about 200 protein factors and 80 small nucleolar RNAs (snoRNAs) (13–16). These factors likely assure the needed speed, accuracy and directionality of the ribosome assembly process (17). The consequences for ribosome synthesis due to loss-of-function mutations in most of these factors have been well described (5,10,11). Moreover, proteomic approaches have revealed several distinct, successive pre-ribosomal particles. The study of the RNA and protein composition of different purified pre-ribosomal complexes is consistent with the presence of distinct intermediates that move from the nucleolus to the nucleoplasm and from there to the cytoplasm (15,18–25). These intermediates are termed, according to their position in the ribosome assembly

*To whom correspondence should be addressed. Tel: +34 95 455 71 06; Fax: +34 95 455 71 04; Email: jdlcd@us.es

pathway and consistently with pioneer work by sucrose gradient analyses (26), 90S pre-ribosomal particles, nuclear and cytoplasmic 43S pre-ribosomal particles and early, medium, late and cytoplasmic pre-60S r-particles (15,16,27) (for an outline, see Supplementary Figure S2A). Apparently, the complexity of the different pre-ribosomal particles decreases during their maturation to r-subunits while concomitant structural rearrangements allow the stable incorporation of all r-proteins (15,16,28). Insights into the approximate timing of association and dissociation of some of the protein ribosome biogenesis factors have been obtained by studying the composition of distinct purified pre-60S complexes from wild-type (15,17) and mutant strains blocked at early, medium or late nuclear steps of ribosome maturation [e.g. see (29,30) and references therein].

It has also long been clear that both the pre-rRNAs (transcribed spacers and mature rRNA sequences) and r-proteins are essential for the pre-rRNA processing events and hence for eukaryotic ribosome synthesis (31–33). A systematic analysis of the role of yeast 40S r-proteins in maturation and transport of 43S pre-ribosomal particles has been performed (34). Recently, an equivalent approach has allowed the analyses of the role of 26 essential yeast 60S r-proteins (35). Before this analysis, the contribution to ribosome biogenesis of only few 60S r-proteins has been studied in detail (36–41). Moreover, the course of the assembly of the r-proteins has not been reported with sufficient precision, mainly due to the fact that r-proteins are common contaminants in purified complexes, therefore it has been difficult to distinguish between unspecific and specific association of r-proteins to pre-ribosomal particles (42,43). Low resolution pictures of early and late r-protein assembly has been obtained by monitoring the kinetics of *in vivo* incorporation of labelled r-proteins into pre-ribosomal particles and cytoplasmic ribosomes in both yeast and HeLa cells (44,45). More recent investigations have analysed the incorporation of tagged yeast 40S r-proteins into 90S and 43S pre-ribosomal particles (46), which have allowed the identification of some principles governing the assembly of the 40S r-subunits and the establishment of a certain parallelism between the *in vivo* assembly of 40S r-subunits and the *in vitro* reconstitution data of bacterial 30S r-subunits (46). Unfortunately, an equivalent analysis of the incorporation of yeast 60S r-proteins into pre-ribosomal particles is still missing.

We are interested in understanding the contribution of specific 60S r-proteins to ribosome biogenesis (38,41). In this study, we have undertaken the functional analysis of yeast L35 in ribosome synthesis. Eukaryotic L35 shares a notable sequence identity with archaeal and eubacterial L29, although L35 carries a specific C-terminal extension (Ribosomal Protein Gene Database, http://ribosome.med .miyazaki-u.ac.jp/ and Supplementary Figure S3). L35 is located close to L25 and L26, thus flanking the nascent peptide exit tunnel (Supplementary Figure S4) in a similar fashion as their respective archaeal and eubacterial L29, L23 and L24 counterparts (47). L35 together with L25 may function as a general docking site for nascent poly-peptide chain-associated factors, such as N-terminal

processing and modification enzymes, chaperones, the signal recognition particle (SRP) and the Sec61/translocon complex (48,49). Regarding ribosome synthesis, it has been suggested by polysome profile analyses that L35 is required for 60S r-subunit accumulation (50). Our results show that L35 is indeed required for the normal accumulation of 60S r-subunit since defective production of L35 causes defects in pre-rRNA processing of $27SA_3$ and $27SB_{L/S}$ and in intra-nuclear transport and nuclear export of pre-60S r-particles. Moreover, we show that L35 assembles in the nucle(ol)us and stably interacts with 27S pre-rRNAs, therefore suggesting that it is added early in the assembly pathway. It has been suggested that zebrafish *RPL35*, as many other r-protein genes, acts as an haploinsufficient tumor suppressor by an as yet unknown mechanism (51). In this study, we also show that depletion of L35 leads to a mild delay in the G1 phase of the cell cycle.

MATERIALS AND METHODS

Strains and microbiological methods

The yeast strains used in this study, which are derivatives of strain BY4741 (52), are listed in Supplementary Table S1. Strains RBY138 and RBY139 are haploid segregants of Y23889 and Y23834 (Euroscarf), respectively. Growth and handling of yeast and standard media were according to established procedures (53,54). Antibiotic-containing plates were prepared by adding the drugs from stock solutions into 2% rich glucose medium (YPD) before pouring the plates. Tetrad dissections were performed using a Singer MS micromanipulator. *Escherichia coli* DH5α strain was used for common cloning and propagation of plasmids (55).

Plasmids

The relevant information on the construction of the different plasmids used in this study can be found in the Supplementary Data. The sequences of oligonucleotides used for the construction of plasmids are listed in Supplementary Table S2. Other plasmids used are described throughout the text. All plasmids used in this study are listed in Supplementary Table S3.

Construction of a *GAL::RPL35* allele and *in vivo* depletion of L35

RBY138 [YCplac33-RPL35A] was crossed to RBY168 [YCplac111], the resulting diploid was sporulated and tetrads were dissected. G418-resistant spore clones from at least three complete non-parental ditypes were transformed with pAS24-RPL35A, which allows expression of N-terminally HA-tagged L35 under the control of a *GAL* promoter. Transformants were restreaked on synthetic 2% galactose (SGal)-Leu plates and subjected to plasmid shuffling on 5-FOA-containing SGal plates at 30°C. One of these clones, RBY175 [pAS24-RPL35A], also named the *GAL::RPL35* strain, was used for further work.

For *in vivo* depletion of L35, the *GAL::RPL35* strain was grown in 2% rich galactose medium (YPGal) at 30°C until mid-exponential phase (OD_{600} = 0.8), and then, harvested, washed and transferred to YPD. Cell growth was monitored over a period of 18 h, during which the cultures were regularly diluted into fresh YPD medium. As control, the wild-type BY4741 strain was used. At different time points, samples were collected to perform protein and RNA extractions, and polysome analysis.

Sucrose gradient centrifugation

Polysome and r-subunit preparations and analyses were performed as previously described (56) using an ISCO UA-6 system with continuous monitoring at A_{254}.

Protein extractions and western blotting analyses

Total yeast protein extracts were prepared and analysed by western blotting according to standard procedures (55). The rabbit polyclonal anti-L35 (57), anti-L1 (58) and anti-S8 (59) antibodies were gifts from M. Seedorf, F. Lacroute and G. Dieci, respectively.

RNA extractions, northern hybridization and primer extension analyses

RNA extraction, northern hybridization and primer extension analyses were carried out according to standard procedures (53,60). In all experiments, RNA was extracted from samples corresponding to 10 OD_{600} units of exponentially grown cells. Equal amounts of total RNA was loaded on gels or used for primer extension reactions (60). The sequences of oligonucleotides used for northern hybridization and primer extension analyses have been described previously (61) and are listed in Supplementary Table S2. Phosphorimager analysis was performed in a FLA-5100 imaging system (Fujifilm) at the Biology Service (CITIUS) from the University of Seville.

Pulse-chase analysis

Pulse-chase labeling of pre-rRNA was performed exactly as described previously (56), using 100 μCi of [5,6-³H]uracil (Perkin Elmer; 45–50 Ci/mmol) per 40 OD_{600} of yeast cells. Total RNA was extracted as above and 20 000 cpm per RNA sample was loaded on gels and analysed as described in (56).

Fluorescence microscopy

To test pre-ribosomal particle export, the appropriate strains were co-transformed with a pRS316 plasmid harboring a L25-eGFP reporter (62) or a S2-eGFP reporter (59) and a pRS413 plasmid expressing the nucleolar marker Nop1-DsRed [(62); this work]. Then, several transformants were grown to mid-log phase in selective liquid medium, washed, and resuspended in PBS buffer (140 mM NaCl, 8 mM Na_2HPO_4, 1.5 mM KH_2PO_4, 2.75 mM KCl, pH 7.3). When needed, cells were transformed with either the pRS316-*GAL-nmd3Δ100* or the pRS316-*GAL*-NMD3FL plasmid (gifts from A. Jacobson), which harbour a dominant-negative truncation or a wild-type allele of the *NMD3* gene, respectively, under the control of an inducible *GAL* promoter (63). Acquisition was done in a Leica DMR microscope equipped with a DC camera following the instructions of the manufacturer. Digital images were processed with Adobe Photoshop 7.0.

Leptomycin B (LMB) experiments were carried out as described (64) with slight modifications (38); briefly, cells from the AJY1539 strain (a gift from A.W. Johnson) were co-transformed with the pUR34-NLS plasmid (gift from M. Corte-Real), which carried the red fluorescent protein DsRed fused to a nuclear localization signal (NLS) (65) and either pRS315-RPL25-eGFP or YCplac111-RPL35B-eGFP. Transfromants were grown at 30°C in the appropriate synthetic 2% glucose (SD) medium to an OD_{600} of about 0.6. Then, cells from 2 ml culture of selected transformants were concentrated 2-fold in fresh medium and split. LMB (Alexis Biochemicals) in 20% ethanol or 20% ethanol vehicle was added to the cultures at a final concentration of 200 ng/ml LMB-0.16% ethanol or 0.16% ethanol, respectively. Cultures were incubated for 1–3 h and then cells were inspected by fluorescence microscopy as above.

Cell morphology was studied under the brightfield microscope with cells fixed with 70% ethanol whose nuclei where stained with 4′,6-diamidino-2-phenylindole dihydrochloride (DAPI) at 0.5 μg/ml (54).

Affinity purification of L35B-eGFP protein

GFP-tagged L35B protein was precipitated following a one-step GFP-Trap®_A procedure slightly modified from that suggested in the manufacturer's instructions (Chromotek). Briefly, 50 ml of GFP-tagged or untagged negative control cells were grown in SD-Ura medium to an OD_{600} of 0.8, washed with cold water, harvested and concentrated in 500 μl of ice-cold lysis buffer (20 mM Tris–HCl, pH 7.5; 1.5 mM $MgCl_2$; 150 mM CH_3COOK; 1 mM DTT; 0.2% Triton X-100) containing a protease inhibitor cocktail (Complete, Roche). Cells were disrupted by vigurous shaking with glass beads in a Fastprep®-24 (MP Biomedicals) at 4°C and total cell extracts were obtained by centrifugation in a microfuge at the maximun speed (*ca.* 16100× *g*) for 15 min at 4°C. To each of the resulting supernatants 50 μl of GFP-Trap®_A beads, equilibrated with the same buffer, were added and the mixture was incubated for 2 h at 4°C with end-over-end tube rotation. After incubation, the beads were extensively washed three times with 5 ml of the same buffer at 4°C and finally collected. RNA was extracted from the beads and the total cell extracts as exactly described in (66), and the extracted RNA was analysed by northern blotting as above.

Flow cytometry

Cells grown in logarithmic phase to an OD_{600} of 0.1–0.3 were harvested, fixed with 70% ethanol and DNA was stained with propidium iodine as previously described (67). Stained cells were analysed using a Becton Dickinson FACScan flow cytometer using CELL

QUEST software packages to collect and analyse the data (BD Biosciences).

RESULTS

Strains for the phenotypic analysis of the *RPL35* genes

Yeast L35 is an essential small r-protein of 120 amino acids with a predicted mass of 13.9 kDa and a predicted basic pI of 11.36 (*Saccharomyces* Genome Database, www.yeastgenome.org). As most yeast r-protein genes (33,68,69), L35 is encoded by two paralogous genes, *RPL35A* (*SOS1, YDL191W*) and *RPL35B* (*SOS2, YDL136W*), which both localized on the left arm of chromosome IV. As also quite common for yeast r-protein genes (70), their coding regions are interrupted by an intron. The coding regions of these two genes are nearly identical, differing in only 3 nt out of 362, but resulting in no change in the amino acid sequences of the predicted L35A and L35B proteins. On the other hand, the two paralogous genes show no substantial sequence homology in their introns or in their 5′ and 3′-non-coding regions.

Early studies indicated that both *RPL35* genes are required for growth and normal accumulation of 60S r-subunits (50) but no further information is available on the role of L35 in ribosome biogenesis. To characterize in detail the contribution of L35 in ribosome biogenesis, we first studied the phenotypic consequences of the deletion of either the *RPL35A* or the *RPL35B* gene. As shown in Figure 1A, the deletion of the *RPL35A* gene (*Δrpl35A* strain) results in a severe growth defect while the deletion of the *RPL35B* gene (*Δrpl35B* strain) has only a slight effect on the growth rate. In agreement, while the generation time in YPD for the wild-type strain grown at 30°C is 1.4 h, the *Δrpl35A* or *Δrpl35B* mutant strains have a doubling time of 3.6 h and 1.7 h, respectively. Since genome-wide expression data suggest that *RPL35A* might contribute to 56% while *RPL35B* to 44% of total *RPL35* mRNA levels (71), the functional disparity between the two deletion strains could not be totally explained by differences in mRNA expression
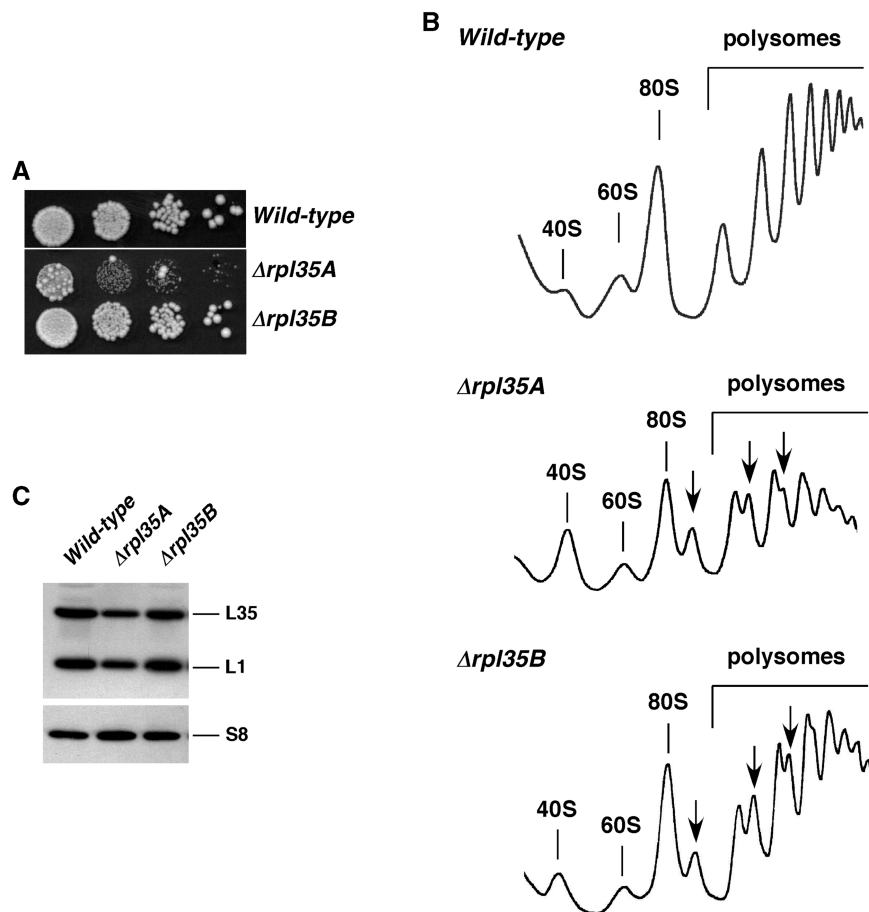

Figure 1. Deletion of either *RPL35A* or *RPL35B* leads to a deficit in 60S r-subunits. (**A**) Growth test of the *rpl35A* and *rpl35B* null mutants compared to their isogenic wild-type control strain. Strains RBY138 (*Δrpl35A*), RBY139 (*Δrpl35B*) and BY4741 (*Wild-type*) were grown in YPD and diluted to an OD$_{600}$ of 0.05. A 10-fold series of dilutions was performed for each strain and 5 μl drops were plated on YPD plates. Plates were incubated at 30°C for 4 days. (**B**) The above strains were grown in YPD at 30°C and harvested at an OD$_{600}$ of 0.8, cell extracts were prepared and 10 A$_{260}$ of each extract were resolved in 7–50% sucrose gradients. The A$_{254}$ was continuously measured. Sedimentation is from left to right. The peaks of free 40S and 60S r-subunits, 80S free couples/monosomes and polysomes are indicated. Half-mers are labelled by arrows. (**C**) Equivalent amounts of the cell extracts described above were subjected to western blot analysis with antibodies against the r-proteins L35, L1 and S8.

levels. To evaluate whether the growth rate of the two deletion strains has any correlation with the L35 protein levels, we examined the polysome profiles of the deletion strains and compared them with that from an isogenic wild-type counterpart. As shown in Figure 1B, both *Δrpl35A* and *Δrpl35B* strains showed a deficit of free 60S versus free 40S r-subunits, a mild decrease in 80S ribosomes and polysomes, and most importantly, an accumulation of half-mer polysomes. Clearly, the *Δrpl35B* strain led to less severe alterations of the profiles than the *Δrpl35A* one. This result suggests that the reduced growth rate of the *Δrpl35A* strain is due to a deficit of 60S r-subunits, which is much larger than the one observed for the *Δrpl35B* strain. To confirm this, we quantified total r-subunits by using run-off and low-Mg^{2+} sucrose gradients. Indeed, in the *Δrpl35A* strain we observed a 25% reduction in the overall quantity of 60S r-subunits relative to the wild-type strain whereas only a 7% reduction was detected in the *Δrpl35B* strain (data not shown). In agreement with this net deficit in 60S r-subunits, western blot analysis indicated that the L35 levels, as well as those of L1 were decreased in the *Δrpl35A* strain, whereas the levels of the small subunit r-protein S8 were not significantly affected. No evident changes were observed in the *Δrpl35B* strain (Figure 1C).

We conclude that the different growth defect observed in the *Δrpl35A* and *Δrpl35B* strains is due to the accompanying deficit in 60S r-subunits in each strain and indicates that *RPL35A* plays a more important role in the production of L35 than does *RPL35B*. Few extra copies of *RPL35B* or *RPL35A*, which were provided from centromeric plasmids, fully restored a wild-type growth rate and polysome profile to the *Δrpl35A* or *Δrpl35B* strains, respectively (Supplementary Figure S5). This suggests that there is no functional distinction between the L35A and L35B proteins at least under standard laboratory conditions when cells are grown in synthetic medium.

Depletion of L35 leads to a strong 60S ribosomal subunit shortage

To study the consequences of the L35 depletion we generated a conditional *GAL::RPL35* strain (see 'Materials and Methods' section). Growth of this strain was identical to that of the isogenic wild-type strain on YPGal plates, showing that the production of N-terminally HA-tagged L35A derived from the *GAL-RPL35A* construct ensures wild-type growth (Figure 2A). As expected, only very residual growth of this strain was observed on YPD plates (Figure 2A). After shifting a mid-logarithmic culture of *GAL::RPL35*
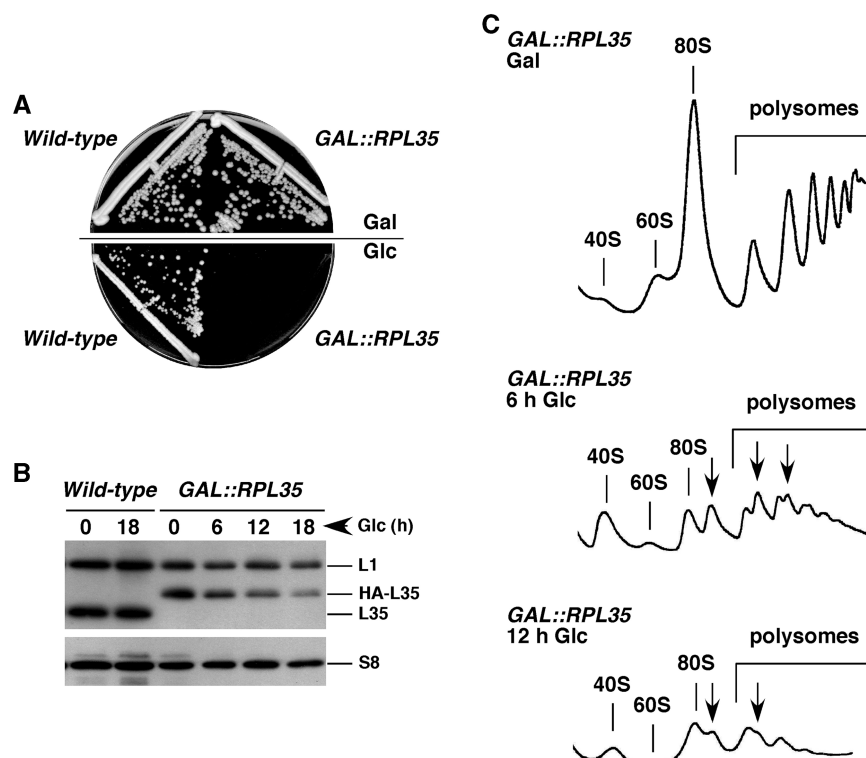

Figure 2. Depletion of L35 results in a deficit in 60S r-subunits. (**A**) Growth comparison of the strains BY4741 (*Wild-type*) and RBY175 (*GAL::RPL35*). The cells were grown in YPGal and streaked on YPGal (Gal) and YPD (Glc) plates, which were incubated at 30°C for 3 days. (**B**) The above strains were grown in YPGal at 30°C and shifted to YPD. Cells were harvested at the indicated times after the shift and cell extracts were prepared. Equivalent amounts of cell extracts were subjected to western blot analysis with antibodies against the r-proteins L35, L1 and S8. (**C**) 10 A$_{260}$ of cell extract from the *GAL::RPL35* strain grown in YPGal (Gal) or shifted for 6 h (6 h Glc) or 12 h (12 h Glc) to YPD were subjected to polysome analysis in 7–50% sucrose gradients. The peaks of free 40S and 60S r-subunits, 80S free couples/monosomes and polysomes are indicated. Half-mers are labelled by arrows.

from liquid YPGal medium to YPD medium, the growth rate rapidly decrease to a doubling time of >10 h after 12 h in YPD, as compared with the 1.5–2 h for the isogenic wild-type control strain (data not shown). Western blot analysis revealed a marked reduction of L35 in the *GAL::RPL35* cells that coincided with the decrease in the growth rate in YPD medium. Interestingly, L1 is also reduced but to a lesser extent and S8 levels remained practically unaffected during the time-course of the shift (Figure 2B).

To examine the consequences of L35 depletion in ribosome biogenesis, we first analysed polysome profiles from cell extracts of the *GAL::RPL35* strain grown in YPGal or after shifting to YPD. As shown in Figure 2C, this strain showed normal polysome profiles when grown in YPGal, including normal levels of free 40S and 60S r-subunit, 80S and polysomes. However, when shifted for only 6 h to YPD, it showed a clear decrease in the levels of free 60S versus free 40S r-subunits, a strong decrease in the 80S peak and polysome and the appearance of large half-mer polysomes. These features were still more pronounced upon a 12 h shift to YPD (Figure 2C). Wild-type cells showed no alteration in the polysome profile when transferred to YPD (data not shown). Consistently, quantification of total r-subunits by low Mg^{2+} sucrose gradients showed that L35 depletion leads to a 40% reduction of the 60S to 40S r-subunit ratio compared to the wild-type control after 12 h of depletion (data not shown).

Altogether, these results indicate that depletion of L35 leads to a deficit in 60S r-subunits relative to 40S r-subunits.

Depletion of L35 delays rRNA processing at ITS2

To determine whether L35 is required for pre-rRNA processing, we analysed the effects of L35 depletion on the kinetics of rRNA production by [5,6-^{3}H]-uracil pulse-chase labelling experiments. Both the wild-type and *GAL::RPL35* strains were first transformed with an empty YCplac33 plasmid (*CEN, URA3*, see 'Materials and Methods' section) to make them prototrophic for uracil. Then, they were pre-grown in liquid SGal-Ura medium and finally shifted to liquid SD-Ura medium for 8 h. At this time point, the *GAL::RPL35* strain was doubling every *ca.* 8–9 h compared with *ca.* 2 h for the wild-type strain. The cells were pulse-labelled for 2 min, then chased for 5, 15, 30 and 60 min with a large excess of non-radioactive uracil. Total RNA was extracted from each sample and analysed by agarose and acrylamide gel electrophoresis, followed by transfer to nylon membranes and fluorography. In wild-type cells, the 35S precursor was converted rapidly into 32S and then into 27S and 20S species, which were further processed into mature 25S and 18S rRNA, respectively. After 15 min of chase, almost all label was in the mature rRNAs. In contrast, in the L35-depleted strain, synthesis of 25S and 5.8S rRNAs was inhibited relative to synthesis of 18S and 5S rRNAs (Figure 3A and B). Processing of 35S pre-rRNA was delayed since the 35S pre-rRNA could be detected after the pulse and the early chase time points. Consistently, traces of the aberrant 23S species appeared (Figure 3A). Processing of 27SB pre-rRNAs was also slowed since these pre-rRNAs persisted even after the 60 min of chase; as a consequence no labelled 25S and 5.8S rRNA were detected (Figure 3A and B). Pulse-chase analyses were also performed with the *Δrpl35A* and *Δrpl35B* strains. These revealed that the *Δrpl35A* mutation led to similar, albeit milder, effects as those observed upon L35 depletion, while the *Δrpl35B* mutant only showed a slight delay of processing of both 35S and 27SB pre-rRNAs (data not shown). Thus, the deficit in 60S r-subunits upon mutation in or depletion
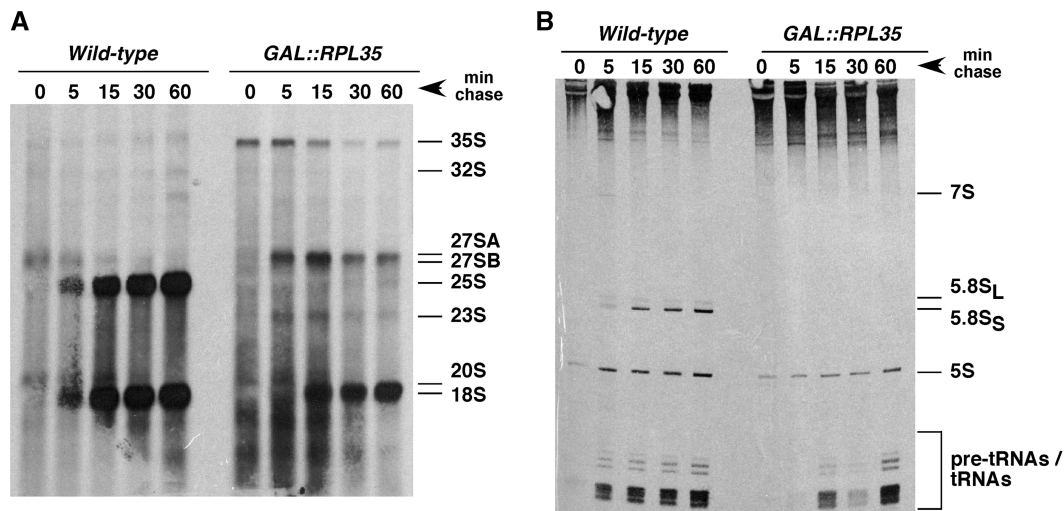

Figure 3. Depletion of L35 impairs 27S pre-rRNA processing. (**A**) Wild-type control strain BY4741 (*Wild-type*) and strain RBY175 (*GAL::RPL35*) were transformed with YCplac33 and then grown at 30°C in SGal-Ura and shifted for 8 h to SD-Ura. Cells were pulse-labelled with [5,6-3H]uracil for 2 min followed by a chase with a large excess of unlabelled uracil for the times indicated. Total RNA was extracted and 20 000 cpm was loaded and separated on (**A**) a 1.2% agarose-6% formaldehyde gel or (**B**) a 7% polyacrylamide-8M urea, transferred to nylon membranes and visualized by fluorography. The positions of the different pre-rRNAs and mature rRNA are indicated.

of L35 is a consequence of impaired 27SB pre-rRNA processing leading to a reduced synthesis of both the mature 25S and 5.8S rRNAs.

Steady-state levels of pre- and mature rRNAs were also analysed by northern hybridization and primer extension. For this, total RNA was extracted from the wild-type and deletion mutants grown in YPD and during a time-course of L35 depletion. As shown in Figure 4A, following deletion of *RPL35A* and L35 depletion, the 35S pre-rRNA and the aberrant 23S species accumulated while 32S, $27SA_2$ and 20S pre-rRNAs decreased. In agreement with the 27SB pre-rRNA persistence seen in pulse chase analyses, steady-state levels of 27SB pre-rRNAs accumulated, while those of 7S pre-rRNA, mature 25S rRNA and to a lesser extent 5.8S rRNA decreased. Some alterations were also detected in the accumulation of mature 18S and 5S rRNAs (Figure 4A and B). The ratio between the long and short forms of mature 5.8S rRNAs was unaltered, suggesting that the alternative 27SA pre-rRNA processing pathways (Supplementary Figure S1) that generate the two 5.8S rRNA species both are impaired. To confirm this, pre-rRNA processing was also assessed by primer extension analysis using an ITS2 probe (Supplementary

Figure S1). As shown in Figure 4C, and consistent with the northern hybridization data, a decrease in the primer extension stop at site A_2 is seen in the *Δrpl35A* and the L35-depleted strains. The $27SA_3$ pre-rRNA, which cannot be readily detected in northern analyses, was accumulated in both the *Δrpl35A* and the L35-depleted strains, as shown by the stop at site A_3. Moreover, as suspected, both $27SB_L$ and $27SB_S$ pre-rRNA were also accumulated upon the deletion of *RPL35A* and the depletion of L35. Finally, primer extension analysis was also performed through site C_2, and the results showed a reduction in the levels of the 25.5S pre-rRNA (data not shown).

Together, these data indicate that L35 is required for proper ITS2 pre-rRNA processing, thus, depletion of L35 strongly impairs cleavage at site C_2. In addition, deletion of *RPL35A* and depletion of L35 delay processing at sites A_0–A_2 and site A_3.

Depletion of L35 impairs export of pre-60S r-particles from the nucleus to the cytoplasm

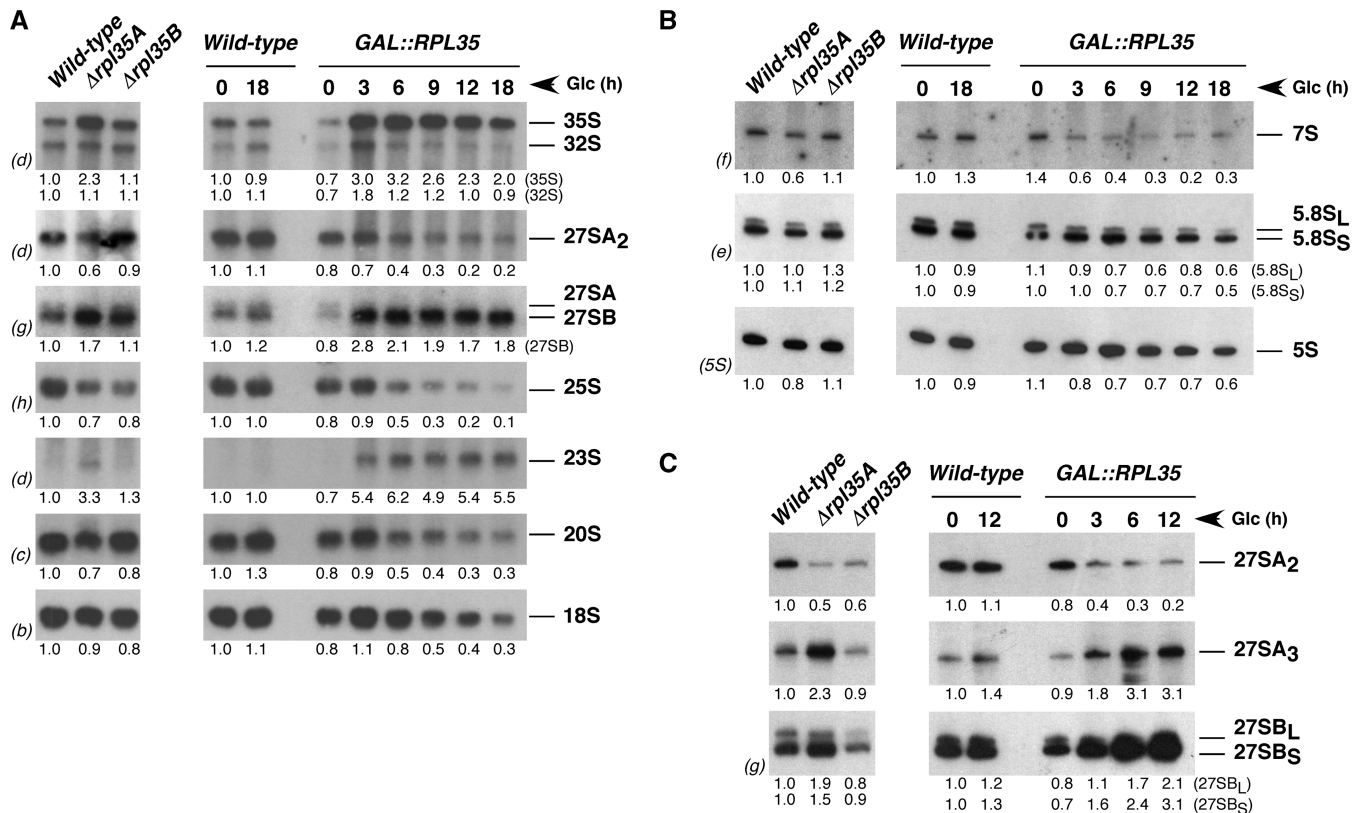To determine whether mutation in or depletion of L35 impairs nuclear export of pre-60S r-particles,

Figure 4. Deletion of *RPL35A* and depletion of L35 affects the steady-state levels of pre-rRNA and mature rRNA species. Strains BY4741 (*Wild-type*), RBY138 (*Δrpl35A*) and RBY139 (*Δrpl35B*) were grown in YPD at 30°C and harvested. BY4741 (*Wild-type*) and RBY175 (*GAL::RPL35*) were grown in YPGal at 30°C, shifted to YPD and harvested at the indicated times. Total RNA was extracted of each sample. Equal amount of total RNA (5 µg) was subjected to northern hybridization or primer extension analysis. (**A**) Northern analysis of high-molecular-mass pre-rRNAs and mature rRNAs. (**B**) Northern analysis of low-molecular-mass pre-rRNAs and mature rRNAs. Probes, between parentheses, are described in Supplementary Figure S1A. (**C**) Primer extension analysis with probe g within ITS2 allows detection of $27SA_2$, $27SA_3$ and both 27SB pre-rRNAs. Signal intensities were measured by phosphorimager scanning; values (indicated below each lane) were normalized to those obtained for the wild-type control grown either in YPD or YPGal, arbitrarily set at 1.0.

we analysed the localization of the 60S reporter L25-eGFP (62) in the different strains used in this study. Under permissive culture conditions (SGal-Ura), L25-eGFP was, as expected for a r-protein, excluded from the vacuole and found predominantly in the cytoplasm in the *GAL::RPL35* strain. However, following a shift to non-permissive conditions (SD-Ura) for as short as 3 h, L25-eGFP accumulated in the nucleus in about 80–90% of the ca. 120 *GAL::RPL35* cells examined (Figure 5A). In most cells, the fluorescence signal was restricted to the nucleolus, which was detected with the nucleolar marker Nop1-DsRed (62) (see magnification in Figure 5B). This phenotype is more evident after 9 h depletion where the fluorescence signal was almost lost from the cytoplasm and prominent all over the nucleus without evident restriction to the nucleolus (Figure 5A). We did not observe nuclear accumulation of the L25-eGFP reporter in the wild type control strain grown in identical conditions (data not shown). Moreover, no accumulation of nuclear fluorescence was observed upon L35 depletion when we studied the localization of the 40S r-subunit reporter S2-eGFP (59) either in galactose or in glucose medium (Figure 5A).

Similar fluorescence microscopy analyses were also performed with the *Δrpl35A* and *Δrpl35B* strains. These revealed that both the L25-eGFP and the S2-eGFP reporters were found in the cytoplasm of all the strains tested.
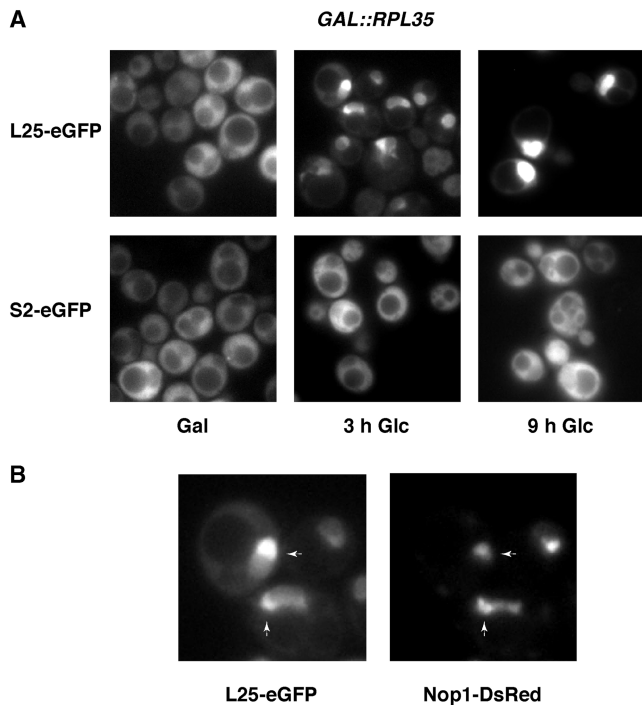

A

GAL::RPL35

L25-eGFP

S2-eGFP

Gal   3 h Glc   9 h Glc

B

L25-eGFP   Nop1-DsRed

Figure 5. Depletion of L35 leads to nuclear retention of the 60S r-subunit reporter L25-eGFP. (**A**) RBY175 (*GAL::RPL35*) cells expressing either L25-eGFP or S2-eGFP were grown in SGal-Ura at 30°C, shifted to SD-Ura for up to 9 h. The GFP signal was analyzed by fluorescence microscopy. (**B**) Magnified picture of selected *GAL::RPL35* cells expressing L25-eGFP and the nucleolar marker Nop1-DsRed, which were depleted for 9 h in SD-Ura. Arrows point to nucleolar fluorescence.

However, we observed a mild nuclear retention of the fluorescence signal of the L25-eGFP reporter in the *Δrpl35A* mutant (data not shown).

We conclude that both intra-nuclear and nucleocytoplasmic transport of pre-60S r-particles is impaired upon defective production of L35. These stalled pre-60S particles most likely contain, besides the stably assembled Rpl25-eGFP, 27SB pre-rRNAs, which are the most obvious pre-rRNAs that accumulated upon deletion of *RPL35A* and L35 depletion. This impairment is apparently specific as transport of pre-40S r-particles is unaffected upon depletion of L35.

L35B assembles in the nucleus

Assembly of r-subunits occurs mainly in the nucle(ol)us, although few 60S r-proteins appears to stably load only with cytoplasmic pre-60S r-particles, such as L24 (30,45) or preferentially with them, such as L10 or P0 (38,72–75). No information was available on the course of the incorporation of L35 into pre-60S r-particles, although we suspect it should occur into the nucleus since several bipartite nuclear localization sequences can be predicted with the cNLS mapper programme (76).

To test whether L35 assembles in the nucleus, we made use of a fully functional L35B-eGFP (Supplementary Figure S5). We first monitored the localization of L35B-eGFP in a LMB sensitive strain (64). This sensitivity is due to the presence of the T539C mutation in the exportin Crm1/Xpo1 (77). Treatment of the sensitive strain with LMB impairs export of pre-ribosomal particles and causes their accumulation in the nucleus (62,78). As shown in Figure 6A, the L25-eGFP, as expected for a r-protein, was primarily localized in the cytoplasm in untreated cells and, as reported (62,78), was readily trapped in the nucleus after a treatment with LMB for 3 h. As also shown in Figure 6A, L35B-eGFP localized similarly as L25-eGFP, indicating that it accumulated in the nucleus only after the LMB treatment. Similar nuclear accumulation was observed upon overexpression of the dominant negative *nmd3Δ100* allele (78) in cells expressing either the L25-eGFP or the L35B-eGFP reporter (Figure 6B) but not upon overexpression of a wild type *NMD3* allele (data not shown). Nmd3 is the Crm1-dependent adapter for export of pre-ribosomal particles through the nuclear pores (78). The dominant negative Nmd3Δ100 protein traps pre-60S r-particles in the nucleus (78).

Altogether, these data strongly suggest that L35B assembles in nucle(ol)ar pre-60S r-particles.

L35 associates with earliest pre-60S ribosomal particles

To address the timing of the nucle(ol)ar L35 assembly, we affinity purified L35B-eGFP containing complexes with GFP-Trap beads (see 'Materials and Methods' section) and analysed which pre-rRNA species were present in these complexes by northern blot hybridization. As shown in Figure 7, and as expected for a 60S r-protein, there was a significant co-purification of mature 25S, 5.8S and 5S rRNAs with L35B-eGFP. We believe that the
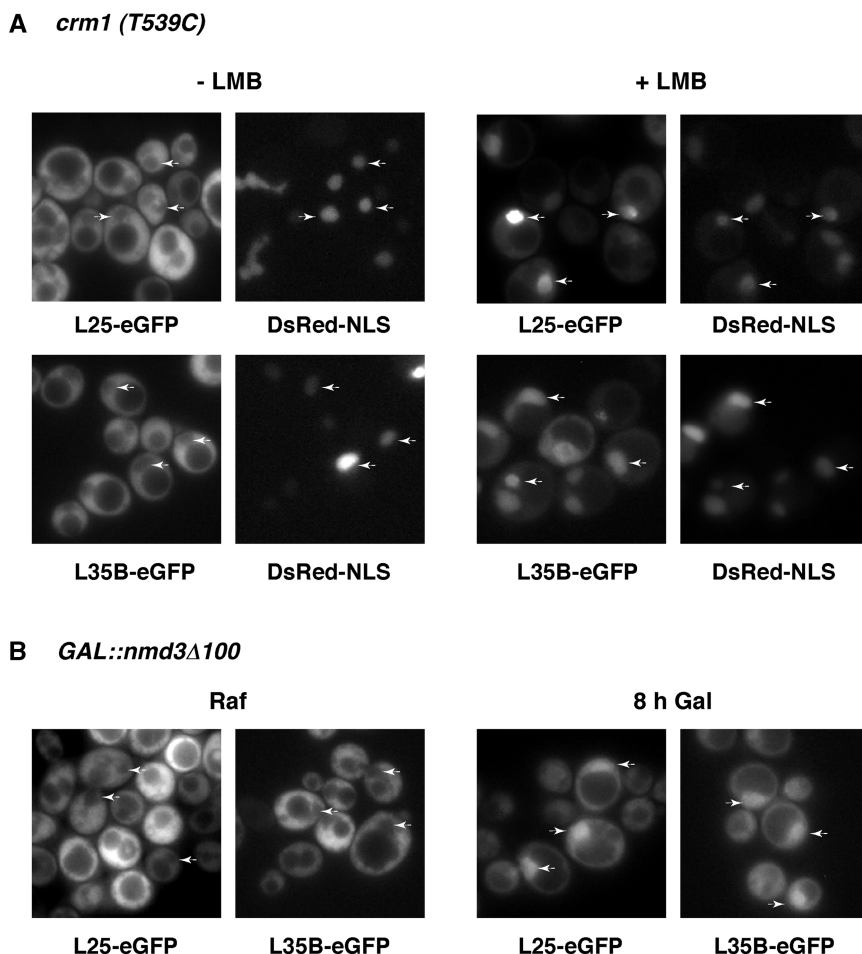
A *crm1 (T539C)*

Figure 6. L35B assembles in the nucleus as inferred upon inhibition of export of 60S pre-ribosomal particles. (**A**) Localization of L25-eGFP and L35B-eGFP in a LMB sensitive strain. Either L25-eGFP or L35B-eGFP was expressed in AJY1539 cells, which harbours the LMB sensitive *crm1 (T539C)* allele. Cells were incubated for 3 h at 30°C in the absence (-LMB) or presence of 200 ng/ml LMB (+LMB). The GFP signal was inspected by fluorescence microscopy. Arrows point to nuclear fluorescence. (**B**) Localization of L25-eGFP and L35-eGFP upon induction of a *nmd3* dominant negative allele. *Δrpl35B* cells expressing L25-eGFP or L35B-eGFP were transformed with the pRS316-*GAL-nmd3Δ100* plasmid and transformants were grown in the presence of raffinose (Raf, SRaf-Leu-Ura medium). Then, galactose was added to fully induce the Nmd3Δ100 protein. The GFP signal was inspected by fluorescence microscopy at the time indicated. Arrows point to nuclear fluorescence.

apparent lack of stochiometry observed for the purification efficiency of 25S versus 5.8S and 5S rRNAs is due to the use of different gel matrices for their resolution. Moreover, mature 18S rRNA was also efficiently co-purified with L35B-eGFP. This must reflect the common unspecific association of 40S with 60S r-subunits in 80S couples in Mg^{2+} containing buffers or ribosomes engaged in translation. Interestingly, purification of L35B-eGFP yielded all precursors (27S and 7S pre-rRNAs) of 25S and 5.8S (Figure 7). Significantly, quantification analysis indicated that all these pre-rRNAs are enriched to similar extents in the L35B-eGFP purified samples. In clear contrast, only background levels were detected for 35S and 20S pre-rRNAs. All these results are specific since no RNAs were detected upon affinity purification from extracts of the untagged strain (Figure 7).

We conclude that L35B does not noticeably associate with 90S pre-ribosomal particles but is stably assembled into very early pre-60S r-particles.

Depletion of L35 leads to cell-cycle delay at the G1 phase

Recent studies indicate that the cell cycle can be impaired at different stages upon mutational inactivation or depletion of individual yeast ribosome synthesis factors and r-proteins [e.g. see (27,41,79–81)]. To study the contribution of L35 to cell-cycle progression, we analysed the cell-cycle status and the cellular morphology of the *GAL::RPL35* and a isogenic wild-type strain under both permissive and non-permissive conditions. First, asynchronous wild-type cells were grown in YPGal medium and shifted for up to 12 h to YPD medium and then the DNA content was analysed by FACS sorting. We detected two nearly equal peaks corresponding to cells with unreplicated (1C) and duplicated genomes (2C) (Figure 8A). A similar pattern was observed for the *GAL::RPL35* cells grown in YPGal medium (Figure 8A). However, after a 3-h shift to YPD, the 1C peak of *GAL::RPL35* cells was slightly higher than the one of 2C. Notably, the imbalance between the 1C and
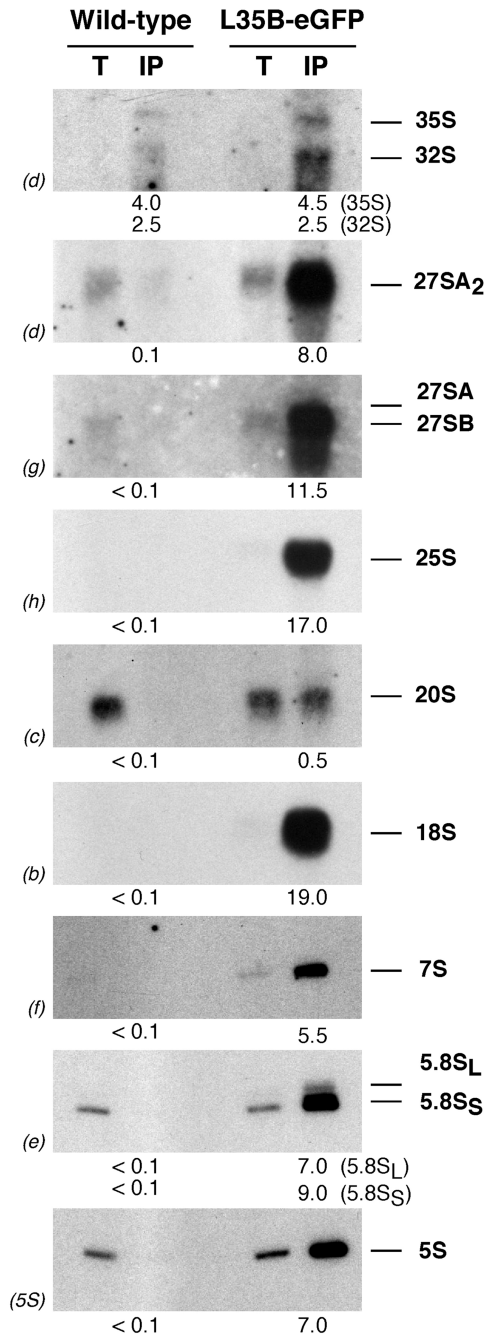
Wild-type **L35B-eGFP**

| T | IP | T | IP |

(d) — 35S
— 32S

4.0   4.5 (35S)
2.5   2.5 (32S)

(d) — 27SA₂

0.1   8.0

(g) — 27SA
— 27SB

< 0.1   11.5

(h) — 25S

< 0.1   17.0

(c) — 20S

< 0.1   0.5

(b) — 18S

< 0.1   19.0

(f) — 7S

< 0.1   5.5

(e) — 5.8S_L
— 5.8S_S

< 0.1   7.0 (5.8S_L)
< 0.1   9.0 (5.8S_S)

(5S) — 5S

< 0.1   7.0

Figure 7. L35B associates with all pre-60S ribosomal particles. L35B-eGFP was affinity purified from total cellular extracts of *Δrpl35B* cells expressing L35B-eGFP with GFP-Trap®_A beads as indicated in 'Materials and Methods' section. Wild-type cells, which express untagged L35B, serves as a negative control. RNA was extracted from the pellets obtained after purification (lanes IP) or from an amount of total extract corresponding to 1/100 of that used for purification (lanes T) and subjected to northern analysis of pre-rRNAs and mature rRNAs. Probes, between parentheses, are described in Figure S1A. Signal intensity was measured by phosphorimager scanning; values (below each IP lane) refer to as the percentage of each RNA recovered after purification.

2C peak was more pronounced after a 12-h shift to YPD, which led to an increase in the 1C/2C area peak from 0.7 in YPGal to 1.4 after the 12 h-shift to YPD (Figure 8A).

Microscopy inspection of DAPI-stained cells from the wild-type grown either in YPGal or shifted to YPD revealed normal cellular morphology and a mixture of unbudded cells (∼43% from ∼120 examined cells) and cells with variably sized buds (Figure 8B). Similar results were obtained for the *GAL::RPL35* cells grown in YPGal medium. However, when the *GAL::RPL35* cells were transferred to YPD medium, a progressive increase in the percentage of unbudded cells was observed, and after 12 h in YPD, about 65% cells from ca. 200 examined cells were small and unbudded (Figure 8B). Similar FACS sorting and microscopy analyses were also performed with the *Δrpl35A* and *Δrpl35B* strains. These revealed similar although slighter phenotypes than those of L35 depleted cells for only the *Δrpl35A* mutant (data not shown).

We conclude that the G1 phase of cell cycle is mildly delayed upon decreased production of L35.

DISCUSSION

In this work, we have addressed the role of yeast L35 r-protein in ribosome biogenesis. L35 is an evolutionarily conserved protein in eukaryotes; moreover, a notable sequence homology exists between the N-terminal and central sequences of L35 and the eubacterial and archaeal L29 (Supplementary Figure S3). According to the X-ray crystals of 50S r-subunits, prokaryotic L29 is a globular protein made up of helical bundle domain [(47); Supplementary Figure S4]. The analysis of the models derived from the cryo-electron microscopy data of the yeast and dog 60S r-subunits suggests that at least the N-terminal and central parts of L35 are structurally similar to prokaryotic L29 (3,4,47); however, the distinct C-terminal extension of L35 can not been modelled. In addition, prokaryotic L29 and eukaryotic L35 have been mapped very close to prokaryotic L23 and L24 and eukaryotic L25 and L26, respectively, surrounding the nascent polypeptide exit tunnel ((3,4,47); Supplementary Figure S4). Due to this fact, L25 and L35 have been shown to be important for the contact of the ribosome with ribosome-associated enzymes, chaperones and complexes such as SRP or the Sec61/translocon (48,49). Finally, the 60S r-subunit models also reveal that L35 might bind mature 5.8S rRNA at equivalent positions to those archaeal L29 interacts in mature 23S rRNA within domain I [(47); Supplementary Figure S6]. Accordingly, it has been demonstrated that rat liver L35 binds *in vitro* to yeast 5.8S rRNA (82).

Unfortunately, despite all this knowledge, there is almost no information available on the role of L35 or its prokaryotic L29 counterpart in ribosome biogenesis, excluding some polysome profiles obtained for the *Δrpl35A* and *Δrpl35B* strains (50). Herewith, we have analysed the consequences for ribosome biogenesis of either the deletion of *RPL35A* and *RPL35B* or the depletion of L35. Our results show that deletion of *RPL35A* leads to a severe impairment of growth while deletion of *RPL35B* has almost no effect on growth (Figure 1). This situation is similar to that found for other many yeast
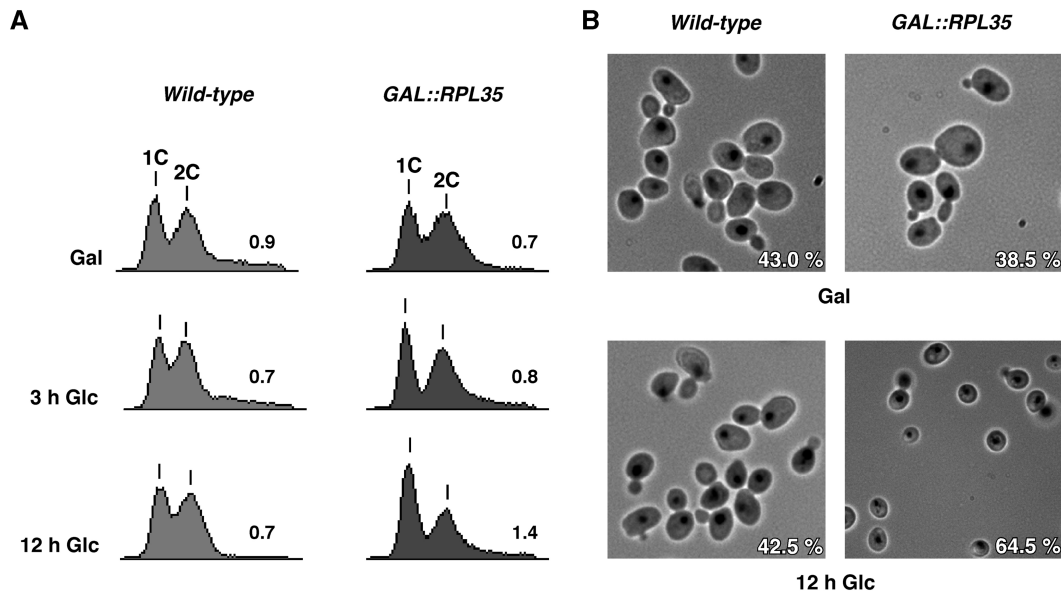
A

B

Figure 8. Depletion of L35 leads to a mild delay of the cell cycle at the G1 phase. (**A**) FACS analysis of unsynchronized cells from the BY4741 (*Wild-type*) or the RBY175 (*GAL::RPL35*) strains. Cells were grown in YPGal (Gal) or shifted for up to 12 h to YPD (Glc) at 30°C. 1C and 2C peaks correspond to cells with unreplicated and duplicated genomes, respectively. Numbers refers to the 1C/2C area peak ratios (**B**) Cell morphology of the wild-type and *GAL::RPL35* cells. Cells were stained with DAPI for localization of nuclei and then visualized by fluorescence and visible phase contrast microscopy. Only merged images are shown. Numbers refer to mean percentages of unbudded cells after three independent experiments.

r-proteins encoded by duplicated genes, among them L15 (83), L11 (84) and L2 (85). In agreement with the previous report (50), polysome analysis reveals a more drastic 60S r-subunit deficit for the *Δrpl35A* than for the *Δrpl35B* strain. Consistent with this, western blot analysis suggests that *RPL35A* plays a more important role in the production of L35 than *RPL35B* (Figure 1). As expected, depletion of L35 leads to an even stronger deficit in 60S r-subunits (Figure 2). Analysis of pre-rRNA processing by pulse-chase labeling and northern blotting analysis clearly indicates that the 60S r-subunit deficit exhibited by the *rpl35* mutants is due to a strong inhibition of processing of the 27SB pre-rRNAs, which leads to reduced formation of 7S and 25.5S pre-rRNAs and thus of mature 5.8S and 25S rRNAs, respectively (Figures 3, 4 and data not shown). Pulse-chase and northern blot analysis also indicate that deletion of *RPL35A* and depletion of L35 cause a decrease in the efficiency of processing at the early cleavage sites A_0, A_1 and A_2, thereby affecting the levels of mature 18S rRNA and its 20S precursor and leading to the appearance and accumulation of the aberrant 23S pre-rRNA (Figures 3 and 4). This type of defect in 18S rRNA synthesis, which has been extensively reported, is a feature of many mutants in genes encoding 60S r-subunit synthesis factors or 60S r-proteins (5,11,41,86). Northern and primer extension analysis also show an accumulation of $27SA_3$ pre-rRNA in the *Δrpl35A* and the L35-depleted strain, however, the ratio of the mature $5.8S_L$ and $5.8S_S$ rRNAs is not altered as observed upon mutation or depletion of RNase MRP, which is the endonuclease responsible for the cleavage at site A_3 (87,88). These pre-rRNA processing defects, at least the accumulation of 27SB pre-rRNAs, closely resemble those described upon

mutation in or depletion of some 60S r-subunit biogenesis factors, such as Dbp10 (89), Mak11 (90), Nip7 (91), Nog1 (30), Nop2 (92), Nop3 (93), Rlp24 (30), Spb1 (94) and Spb4 (95). The levels of $27SA_3$ pre-rRNAs were checked only upon depletion of Spb1 and Spb4 and in both cases, similarly as upon L35 depletion, there was a clear increase of this precursor, especially at early depletion time points (94,95). Interestingly, depletion of r-protein L25 as well as mutations in either the L25-binding site within domain III of 25S rRNA or in L25, which abolish its association with this rRNA site also resulted in a notable inhibition of 27SB pre-rRNA processing (40,96,97). Peculis and co-workers have also demonstrated that formation of the so-called ITS2 proximal stem in which the 3′-end of 5.8S rRNA base-pairs with the 5′-end of 25S rRNA is a prerequisite for efficient 27SB pre-rRNA processing (32,98,99). All these results and observations strongly suggest that assembly of L25 and/or L35 may be required to achieve the proper structural conformation in the ITS2 region of the 27SB-preRNAs for efficient cleavage at site C_2. Nevertheless, it is unlikely that L35, which lacks known nuclease motifs, represents the still unknown endonuclease responsible for this cleavage. Further experiments are required to identify this endo-nuclease and test its link with L25 and L35 and factors such as Spb4 that are required for 27SB pre-rRNA processing; one possibility is that interaction of any of these factors with 27SB pre-rRNA containing pre-60S r-particles could be dependent on previous association of L25 and L35 r-proteins. Recently, it has been proposed that 20S to 18S pre-rRNA processing by endonucleolytic cleavage at site D is promoted by a structural rearrangement of cytoplasmic 43S pre-ribosomal particles (100). This requires, in addition to the endonuclease Nob1 and

the RNA helicase Prp43 (100), the participation of S3 (28,34) and the C-terminal end of S14 (101) among other 40S r-proteins such as S0, S2, S10, S15, S20, S21, S26 and S28, which all are needed for efficient 20S pre-rRNA processing to mature 18S (34,102). We wonder if a similar scenario would apply for the function of r-proteins L25 and L35, the C_2-site endonuclease and the RNA helicases Spb4 and Dpb10.

In addition to pre-rRNA processing defects, very rapidly upon L35 depletion and in *Δrpl35A* cells, there is an accumulation of the L25-eGFP but not of the S2-eGFP reporter first in the nucleolus and later in the whole nucleus (Figure 5). This result suggests that L25-GFP containing pre-60S r-particles are being retained in the nucle(ol)us due to impaired intra-nuclear and nucleo-cytoplasmic export. This phenotype has previously been observed in several mutants affecting 60S r-subunit biogenesis [e.g. see (103) and references therein], including some mutants of 60S r-protein genes (38,41,62). As earlier discussed (103), this phenotype is likely not the consequence of a defect in the *bona fide* export machinery but of a quality control system that retains defective pre-60S r-subunit particles. L25 has been suggested to assemble at an early stage of the 60S r-subunit maturation pathway (45), thus since the *rpl35* mutants accumulate 27SB pre-rRNAs, the L25-eGFP fluorescence signal observed at early time points of L35 depletion would mainly correspond to nucleolar, aberrant early E_2 pre-60S r-particles. This is consistent with the fact that 27SB pre-rRNA processing at site C_2 most likely occurs in the nucleolus (23,104). Export of pre-60S r-particles requires the participation of several nuclear export receptors among them Arx1 (105,106). Results of Johnson's laboratory strongly suggest that Arx1 binds in the vicinity of L25 and L35 at the exit tunnel of late pre-60S r-particles (107). This is consistent with the fact that Arx1 is structurally related to methionine aminopeptidases, which as mentioned above, interact with translating ribosomes *via* the outside part of the nascent peptide exit tunnel (48). Therefore, some of the accumulation of L25-eGFP in the nucleoplasm, seen in the L35-depleted strain at late time points, could reflect the loss of Arx1 binding to aberrant pre-60S r-particles. Indeed, our initial experiments show that the sedimentation behavior of Arx1 is altered upon L35-depletion. Thus, in the *GAL::RPL35* strain in permissive conditions, Arx1 co-sediments with both free fractions and large complexes that could correspond to pre-60S r-particles in sucrose gradients. However, upon L35-depletion, Arx1 is largely absent from the 60S peak and is predominantly present at the top of the gradient. This suggests that Arx1 binding to pre-60S r-particles depends on the presence of L35 in these r-particles (R.B., unpublished results).

In this work, we have also addressed the course of assembly of L35. No previous information was available for the yeast L35 r-protein even in the seminal work that addressed the kinetics of stable association of most r-proteins with pre-ribosomal particles (45). However, it could be demonstrated that human L35 r-protein binds to nucle(ol)ar pre-60S r-particles in HeLa cells (44). Consistently, it has also been shown in HeLa cells that L35 is imported to the nucleus due to the presence of a NLS within the C-terminal part of the protein (108). In this study, we present several lines of evidence that yeast L35 assembly occurs in the nucle(ol)us. Thus, we show that a functional GFP-tagged L35B protein accumulates in the nucleus upon inhibition of nucleo-cytoplasmic export of pre-60S r-particles (Figure 6), either by a LMB treatment or overexpression of the *nmd3Δ100* allele. We have also examined the pre- and mature rRNAs with which affinity-purified L35B-eGFP is associated (Figure 7). Our results strongly suggest that L35 is not present in 90S pre-ribosomal particles and it only stably binds to early pre-60S r-particles as soon as 27SA$_2$ pre-rRNA is formed. These results are consistent with the fact that only few 60S r-subunit biogenesis factors and r-proteins have been detected in TAP-purifications of components of 90S pre-ribosomal particles (18). In *E. coli*, L29, the bacterial counterpart of yeast L35, is also an early assembling r-protein (109,110). Strikingly, binding of L29 to 23S rRNA *in vitro* is strongly dependent on L4, which lacks a known eukaryotic counterpart, and L23 and L24, which are the bacterial homologues of L25 and L26, respectively (Ribosomal Protein Gene Database, http://ribosome.med.miyazaki-u.ac.jp). As above mentioned, yeast L25 and L26 are the closest neighbours of L35 (Supplementary Figure S4), thus, further experiments are required to determine whether *in vivo* assembly of yeast L25, L26 and L35 is interdependent. Supplementary Figure S2 summarizes the conclusions of this study concerning the L35 assembly in wild-type cells and the dynamics of 60S r-subunit maturation upon depletion of this 60S r-protein.

While this manuscript was finalized, Pöll *et al.* (35) reported a comparative analysis of the pre-rRNA processing and nucleo-cytoplasmic transport defects that arise upon depletion of 26 different yeast 60S r-proteins, among them L35. Consistent with our data, it was shown that depletion of L35 strongly delays 27SB pre-rRNA processing into 7S and 25.5S pre-rRNAs and inhibits export of pre-60S r-particles. Interestingly, not only L35 and the expected L25 were found to be required for 27SB pre-rRNA processing, but also L9, L19, L23, L27 and L34 (35). Understanding how all these different 60S r-proteins and L26, which was unfortunately not included in that study (35), do cooperate to promote efficient cleavage at site C_2 clearly requires further work.

Finally, we report that L35 depletion results in small, unbudded cells that are mildly delayed in the G1 phase of the cell cycle (Figure 8). In yeast, cell-cycle defects have been previously described for mutants or strains depleted of r-proteins and biogenesis factors [see (27,41,81) and references therein]. Although, an impairment of different cell-cycle stages could be observed, arrest in the G1 phase was the most common phenotype (41,80,81). This has been generally related to the intimate link between progression through the G1 phase of the cell cycle and active protein synthesis, which is a prerequisite for acquiring the critical cell size and mass in order to pass the Start point (81,111). It has been suggested that zebrafish *RPL35*, as many other r-protein genes, acts as an haploinsufficient

tumor suppressor by a yet unknown mechanism (51). Indeed, the heterozygous zebrafish line containing a loss-of-function mutation in one of the two *RPL35* alleles has the highest predisposition to cancer among the different r-protein genes analysed (51). As previously discussed (17), it seems contradictory that a reduced ribosome synthesis could lead to dysregulation of cell growth and oncogenesis; however, a delayed progression in cell cycle may increase the selective pressure for mutations to overcome the problems of a reduced ribosome production. A challenge for future studies will be to elucidate the molecular mechanisms underlying the connections between ribosome biogenesis defects and cancer development.

SUPPLEMENTARY DATA

Supplementary Data are available at NAR Online.

REFERENCES

1. Steitz,T.A. (2008) A structural understanding of the dynamic ribosome machine. *Nat. Rev. Mol. Cell. Biol.*, **9**, 242–253.
2. Schmeing,T.M. and Ramakrishnan,V. (2009) What recent ribosome structures have revealed about the mechanism of translation. *Nature*, **461**, 1234–1242.
3. Spahn,C.M., Beckmann,R., Eswar,N., Penczek,P.A., Sali,A., Blobel,G. and Frank,J. (2001) Structure of the 80S ribosome from *Saccharomyces cerevisiae*-tRNA-ribosome and subunit-subunit interactions. *Cell*, **107**, 373–386.
4. Chandramouli,P., Topf,M., Menetret,J.F., Eswar,N., Cannone,J.J., Gutell,R.R., Sali,A. and Akey,C.W. (2008) Structure of the mammalian 80S ribosome at 8.7 A resolution. *Structure*, **16**, 535–548.
5. Henras,A.K., Soudet,J., Gerus,M., Lebaron,S., Caizergues-Ferrer,M., Mougin,A. and Henry,Y. (2008) The post-transcriptional steps of eukaryotic ribosome biogenesis. *Cell. Mol. Life Sci.*, **65**, 2334–2359.
6. Gerbi,S.A., Borovjagin,A.V. and Lange,T.S. (2003) The nucleolus: a site of ribonucleoprotein maturation. *Curr. Opin. Cell Biol.*, **15**, 318–325.
7. Udem,S.A. and Warner,J.R. (1973) The cytoplasmic maturation of a ribosomal precursor ribonucleic acid in yeast. *J. Biol. Chem.*, **248**, 1412–1416.
8. Trapman,J., Planta,R.J. and Raué,H.A. (1976) Maturation of ribosomes in yeast. II. Position of the low molecular weight rRNA species in the maturation process. *Biochim. Biophys. Acta*, **442**, 275–284.
9. Gerbi,S.A. and Borovjagin,A.V. (2004) Pre-ribosomal RNA processing in multicellular organisms. In Olson,M.O.J. (ed.), *Nucleolus*. Landes Biosciences/Eurekah.com, Georgetown, pp. 170–198.
10. Kressler,D., Linder,P. and de la Cruz,J. (1999) Protein *trans*-acting factors involved in ribosome biogenesis in *Saccharomyces cerevisiae*. *Mol. Cell. Biol.*, **19**, 7897–7912.
11. Venema,J. and Tollervey,D. (1999) Ribosome synthesis in *Saccharomyces cerevisiae*. *Annu. Rev. Genet.*, **33**, 261–311.
12. Nomura,M., Nogi,Y. and Oakes,M. (2004) Transcription of rDNA in the yeast *Saccharomyces cerevisiae*. In Olson,M.O.J. (ed.), *Nucleolus*. Landes Bioscience/Eurekah.com, Georgetown, pp. 128–153.
13. Henras,A.K., Dez,C. and Henry,Y. (2004) RNA structure and function in C/D and H/ACA s(no)RNPs. *Curr. Opin. Struct. Biol.*, **14**, 335–343.
14. Kiss,T. (2002) Small nucleolar RNAs: an abundant group of noncoding RNAs with diverse cellular functions. *Cell*, **109**, 145–148.
15. Fromont-Racine,M., Senger,B., Saveanu,C. and Fasiolo,F. (2003) Ribosome assembly in eukaryotes. *Gene*, **313**, 17–42.
16. de la Cruz,J., Kressler,D. and Linder,P. (2004) In Olson,M.O.J. (ed.), *Nucleolus*. Kluwer academic. Landes Bioscience/eurekah.com, Georgetown, pp. 258–285.
17. Kressler,D., Hurt,E. and Bassler,J. (2009) Driving ribosome assembly. *Biochim. Biophys. Acta*, doi: 10.1016/j.bbamcr.2009.10.009.
18. Grandi,P., Rybin,V., Bassler,J., Petfalski,E., Strauss,D., Marzioch,M., Schäfer,T., Kuster,B., Tschochner,H., Tollervey,D. *et al.* (2002) 90S pre-ribosomes include the 35S pre-rRNA, the U3 snoRNP, and 40S subunit processing factors but predominantly lack 60S synthesis factors. *Mol. Cell*, **10**, 105–115.
19. Dragon,F., Gallagher,J.E., Compagnone-Post,P.A., Mitchell,B.M., Porwancher,K.A., Wehner,K.A., Wormsley,S., Settlage,R.E., Shabanowitz,J., Osheim,Y. *et al.* (2002) A large nucleolar U3 ribonucleoprotein required for 18S ribosomal RNA biogenesis. *Nature*, **417**, 967–970.
20. Schäfer,T., Strauss,D., Petfalski,E., Tollervey,D. and Hurt,E. (2003) The path from nucleolar 90S to cytoplasmic 40S pre-ribosomes. *EMBO J.*, **22**, 1370–1380.
21. Harnpicharnchai,P., Jakovljevic,J., Horsey,E., Miles,T., Roman,J., Rout,M., Meagher,D., Imai,B., Guo,Y., Brame,C.J. *et al.* (2001) Composition and functional characterization of yeast 66S ribosome assembly intermediates. *Mol. Cell*, **8**, 505–515.
22. Bassler,J., Grandi,P., Gadal,O., Lessmann,T., Petfalski,E., Tollervey,D., Lechner,J. and Hurt,E. (2001) Identification of a 60S preribosomal particle that is closely linked to nuclear export. *Mol. Cell*, **8**, 517–529.
23. Nissan,T.A., Bassler,J., Petfalski,E., Tollervey,D. and Hurt,E. (2002) 60S pre-ribosome formation viewed from assembly in the nucleolus until export to the cytoplasm. *EMBO J.*, **21**, 5539–5547.
24. Milkereit,P., Gadal,O., Podtelejnikov,A., Trumtel,S., Gas,N., Petfalski,E., Tollervey,D., Mann,M., Hurt,E. and Tschochner,H. (2001) Maturation and intranuclear transport of pre-ribosomes requires Noc proteins. *Cell*, **105**, 499–509.
25. Kallstrom,G., Hedges,J. and Johnson,A. (2003) The putative GTPases Nog1p and Lsg1p are required for 60S ribosomal subunit biogenesis and are localized to the nucleus and cytoplasm, respectively. *Mol. Cell. Biol.*, **23**, 4344–4355.
26. Trapman,J., Retèl,J. and Planta,R.J. (1975) Ribosomal precursor particles from yeast. *Exp. Cell Res.*, **90**, 95–104.
27. Dez,C. and Tollervey,D. (2004) Ribosome synthesis meets the cell cycle. *Curr. Opin. Microbiol.*, **7**, 631–637.

28. Schäfer,T., Maco,B., Petfalski,E., Tollervey,D., Bottcher,B., Aebi,U. and Hurt,E. (2006) Hrr25-dependent phosphorylation state regulates organization of the pre-40S subunit. *Nature*, **441**, 651–655.

29. Lebreton,A., Rousselle,J.C., Lenormand,P., Namane,A., Jacquier,A., Fromont-Racine,M. and Saveanu,C. (2008) 60S ribosomal subunit assembly dynamics defined by semi-quantitative mass spectrometry of purified complexes. *Nucleic Acids Res.*, **36**, 4988–4999.

30. Saveanu,C., Namane,A., Gleizes,P.E., Lebreton,A., Rousselle,J.C., Noaillac-Depeyre,J., Gas,N., Jacquier,A. and Fromont-Racine,M. (2003) Sequential protein association with nascent 60S ribosomal particles. *Mol. Cell. Biol.*, **23**, 4449–4460.

31. van Nues,R.W., Venema,J., Rientjes,J.M., Dirks-Mulder,A. and Raué,H.A. (1995) Processing of eukaryotic pre-rRNA: the role of the transcribed spacers. *Biochem Cell Biol*, **73**, 789–801.

32. Côté,C.A., Greer,C.L. and Peculis,B.A. (2002) Dynamic conformational model for the role of ITS2 in pre-rRNA processing in yeast. *RNA*, **8**, 786–797.

33. Woolford,J.L. Jr and Warner,J.R. (1991) The ribosome and its synthesis. In Broach,J.R., Pringle,J.R. and Jones,E.W. (eds), *The Molecular and Cellular Biology of the yeast Saccharomyces: Genome Dynamics, Protein Synthesis, and Energetics*, Vol. 1. Cold Spring Harbor Laboratory Press, Cold Spring Harbor, NY, pp. 587–626.

34. Ferreira-Cerca,S., Poll,G., Gleizes,P.E., Tschochner,H. and Milkereit,P. (2005) Roles of eukaryotic ribosomal proteins in maturation and transport of pre-18S rRNA and ribosome function. *Mol. Cell*, **20**, 263–275.

35. Pöll,G., Braun,T., Jakovljevic,J., Neueder,A., Jakob,S., Woolford,J.L. Jr, Tschochner,H. and Milkereit,P. (2009) rRNA maturation in yeast cells depleted of large ribosomal subunit proteins. *PLoS ONE*, **4**, e8249.

36. Deshmukh,M., Tsay,Y.-F., Paulovich,A.G. and Woolford,J.L. Jr (1993) Yeast ribosomal protein L1 is required for the stability of newly synthesized 5S rRNA and the assembly of 60S ribosomal subunits. *Mol. Cell. Biol.*, **13**, 2835–2845.

37. Deshmukh,M., Stark,J., Yeh,L.C., Lee,J.C. and Woolford,J.L. Jr (1995) Multiple regions of yeast ribosomal protein L1 are important for its interaction with 5 S rRNA and assembly into ribosomes. *J. Biol. Chem.*, **270**, 30148–30156.

38. Rodríguez-Mateos,M., García-Gómez,J.J., Francisco-Velilla,R., Remacha,M., de la Cruz,J. and Ballesta,J.P.G. (2009) Role and dynamics of the ribosomal protein P0 and its related trans-acting factor Mrt4 during ribosome assembly in *Saccharomyces cerevisiae*. *Nucleic Acids Res.*, **37**, 7519–7532.

39. Martín-Marcos,P., Hinnebusch,A.G. and Tamame,M. (2007) Ribosomal protein L33 is required for ribosome biogenesis, subunit joining, and repression of GCN4 translation. *Mol. Cell. Biol.*, **27**, 5968–5985.

40. van Beekvelt,C.A., de Graaff-Vincent,M., Faber,A.W., van't Riet,J., Venema,J. and Raué,H.A. (2001) All three functional domains of the large ribosomal subunit protein L25 are required for both early and late pre-rRNA processing steps in *Saccharomyces cerevisiae*. *Nucleic Acids Res.*, **29**, 5001–5008.

41. Rosado,I.V., Kressler,D. and de la Cruz,J. (2007) Functional analysis of *Saccharomyces cerevisiae* ribosomal protein Rpl3p in ribosome synthesis. *Nucleic Acids Res.*, **35**, 4203–4213.

42. Krogan,N.J., Cagney,G., Yu,H., Zhong,G., Guo,X., Ignatchenko,A., Li,J., Pu,S., Datta,N., Tikuisis,A.P. *et al.* (2006) Global landscape of protein complexes in the yeast *Saccharomyces cerevisiae*. *Nature*, **440**, 637–643.

43. Gavin,A.C., Bosche,M., Krause,R., Grandi,P., Marzioch,M., Bauer,A., Schultz,J., Rick,J.M., Michon,A.M., Cruciat,C.M. *et al.* (2002) Functional organization of the yeast proteome by systematic analysis of protein complexes. *Nature*, **415**, 141–147.

44. Lastick,S.M. (1980) The assembly of ribosomes in HeLa cell nucleoli. *Eur . J. Biochem.*, **113**, 175–182.

45. Kruiswijk,T., Planta,R.J. and Krop,J.M. (1978) The course of the assembly of ribosomal subunits in yeast. *Biochim. Biophys. Acta*, **517**, 378–389.

46. Ferreira-Cerca,S., Poll,G., Kuhn,H., Neueder,A., Jakob,S., Tschochner,H. and Milkereit,P. (2007) Analysis of the *in vivo* assembly pathway of eukaryotic 40S ribosomal proteins. *Mol. Cell*, **28**, 446–457.

47. Klein,D.J., Moore,P.B. and Steitz,T.A. (2004) The roles of ribosomal proteins in the structure assembly, and evolution of the large ribosomal subunit. *J. Mol. Biol.*, **340**, 141–177.

48. Kramer,G., Boehringer,D., Ban,N. and Bukau,B. (2009) The ribosome as a platform for co-translational processing, folding and targeting of newly synthesized proteins. *Nature Struct. Mol. Biol.*, **16**, 589–597.

49. Becker,T., Bhushan,S., Jarasch,A., Armache,J.P., Funes,S., Jossinet,F., Gumbart,J., Mielke,T., Berninghausen,O., Schulten,K. *et al.* (2009) Structure of monomeric yeast and mammalian Sec61 complexes interacting with the translating ribosome. *Science*, **326**, 1369–1373.

50. Zhong,T. and Arndt,K.T. (1993) The yeast SIS1 protein, a DnaJ homolog, is required for the initiation of translation. *Cell*, **73**, 1175–1186.

51. Amsterdam,A., Sadler,K.C., Lai,K., Farrington,S., Bronson,R.T., Lees,J.A. and Hopkins,N. (2004) Many ribosomal protein genes are cancer genes in zebrafish. *PLoS Biol.*, **2**, E139.

52. Brachmann,C.B., Davies,A., Cost,G.J., Caputo,E., Li,J., Hieter,P. and Boeke,J.D. (1998) Designer deletion strains derived from *Saccharomyces cerevisiae* S288C: a useful set of strains and plasmids for PCR-mediated gene disruption and other applications. *Yeast*, **14**, 115–132.

53. Ausubel,F.M., Brent,R., Kingston,R.E., Moore,D.D., Seidman,J.G., Smith,J.A. and Struhl,K. (1994) *Saccharomyces cerevisiae. Current Protocols in Molecular Biology*, Vol. 2. John Wiley & Sons, Inc., New York, NY, pp. 13.10.11–13.14.17.

54. Kaiser,C., Michaelis,S. and Mitchell,A. (1994) *Methods in Yeast Genetics: A Cold Spring Harbor Laboratory Course Manual*. Cold Spring Harbor Laboratory Press, Cold Spring Harbor, NY.

55. Sambrook,J., Fritsch,E.F. and Maniatis,T. (1989) *Molecular Cloning: A Laboratory Manual*, 2nd edn. Cold Spring Harbor Laboratory Press, Cold Spring Harbor, NY.

56. Kressler,D., de la Cruz,J., Rojo,M. and Linder,P. (1998) Dbp6p is an essential putative ATP-dependent RNA helicase required for 60S-ribosomal-subunit assembly in *Saccharomyces cerevisiae*. *Mol. Cell. Biol.*, **18**, 1855–1865.

57. Frey,S., Pool,M. and Seedorf,M. (2001) Scp160p, an RNA-binding, polysome-associated protein, localizes to the endoplasmic reticulum of Saccharomyces cerevisiae in a microtubule-dependent manner. *J. Biol. Chem.*, **276**, 15905–15912.

58. Petitjean,A., Bonneaud,N. and Lacroute,F. (1995) The duplicated *Saccharomyces cerevisiae* gene *SSM1* encodes a eucaryotic homolog of the eubacterial and archeabacterial L1 ribosomal protein. *Mol. Cell. Biol.*, **15**, 5071–5081.

59. Milkereit,P., Strauss,D., Bassler,J., Gadal,O., Kuhn,H., Schutz,S., Gas,N., Lechner,J., Hurt,E. and Tschochner,H. (2003) A Noc-complex specifically involved in the formation and nuclear export of ribosomal 40S subunits. *J. Biol. Chem.*, **278**, 4072–4081.

60. Venema,J., Planta,R.J. and Raué,H.A. (1998) *In vivo* mutational analysis of ribosomal RNA in *Saccharomyces cerevisiae*. In Martin,R. (ed.), *Protein Synthesis: Methods and Protocols*, Vol. 77. Humana Press, Totowa, NJ, pp. 257–270.

61. Rosado,I.V., Dez,C., Lebaron,S., Caizergues-Ferrer,M., Henry,Y. and de la Cruz,J. (2006) Characterization of *Saccharomyces cerevisiae* Npa2p (Urb2p) reveals a low-molecular-mass complex containing Dbp6p, Npa1p (Urb1p), Nop8p, and Rsa3p involved in early steps of 60S ribosomal subunit biogenesis. *Mol. Cell. Biol.*, **27**, 1207–1221.

62. Gadal,O., Strauss,D., Kessl,J., Trumpower,B., Tollervey,D. and Hurt,E. (2001) Nuclear export of 60S ribosomal subunit depends on Xpo1p and requires a nuclear export sequence-containing factor, Nmd3p, that associates with the large subunit protein Rpl10p. *Mol. Cell. Biol.*, **21**, 3405–3415.

63. Belk,J.P., he,F. and Jacobson,A. (1999) Overexpression of truncated Nmd3p inhibits protein synthesis in yeast. *RNA*, **5**, 1055–1070.

64. Hedges,J., West,M. and Johnson,A.W. (2005) Release of the export adapter, Nmd3p, from the 60S ribosomal subunit requires

Rpl10p and the cytoplasmic GTPase Lsg1p. *EMBO J.*, **24**, 567–579.

65. Rodrigues,F., van Hemert,M., Steensma,H.Y., Corte-Real,M. and Leao,C. (2001) Red fluorescent protein (DsRed) as a reporter in Saccharomyces cerevisiae. *J. Bacteriol.*, **183**, 3791–3794.

66. Dez,C., Froment,C., Noaillac-Depeyre,J., Monsarrat,B., Caizergues-Ferrer,M. and Henry,Y. (2004) Npa1p, a component of very early pre-60S ribosomal particles, associates with a subset of small nucleolar RNPs required for peptidyl transferase center modification. *Mol. Cell. Biol.*, **24**, 6324–6337.

67. Winey,M., Goetsch,L., Baum,P. and Byers,B. (1991) *MPS1* and *MPS2*: novel yeast genes defining distinct steps of spindle pole body duplication. *J. Cell. Biol.*, **114**, 745–754.

68. Warner,J.R. (1989) Synthesis of ribosomes in *Saccharomyces cerevisiae*. *Microbiol. Rev.*, **53**, 256–271.

69. Warner,J.R. (1999) The economics of ribosome biosynthesis in yeast. *Trends Biochem. Sci.*, **24**, 437–440.

70. Spingola,M., Grate,L., Haussler,D. and Ares,M. Jr (1999) Genome-wide bioinformatic and molecular analysis of introns in *Saccharomyces cerevisiae*. *RNA*, **5**, 221–234.

71. Holstege,F.C., Jennings,E.G., Wyrick,J.J., Lee,T.I., Hengartner,C.J., Green,M.R., Golub,T.R., Lander,E.S. and Young,R.A. (1998) Dissecting the regulatory circuitry of a eukaryotic genome. *Cell*, **95**, 717–728.

72. Hofer,A., Bussiere,C. and Johnson,A.W. (2007) Mutational analysis of the ribosomal protein Rpl10 from yeast. *J. Biol. Chem.*, **282**, 32630–32639.

73. West,M., Hedges,J.B., Chen,A. and Johnson,A.W. (2005) Defining the order in which Nmd3p and Rpl10p load onto nascent 60S ribosomal subunits. *Mol. Cell. Biol.*, **25**, 3802–3813.

74. Kemmler,S., Occhipinti,L., Veisu,M. and Panse,V.G. (2009) Yvh1 is required for a late maturation step in the 60S biogenesis pathway. *J. Cell. Biol.*, **186**, 863–880.

75. Lo,K.Y., Li,Z., Wang,F., Marcotte,E.M. and Johnson,A.W. (2009) Ribosome stalk assembly requires the dual-specificity phosphatase Yvh1 for the exchange of Mrt4 with P0. *J. Cell. Biol.*, **186**, 849–862.

76. Kosugi,S., Hasebe,M., Tomita,M. and Yanagawa,H. (2009) Systematic identification of cell cycle-dependent yeast nucleocytoplasmic shuttling proteins by prediction of composite motifs. *Proc. Natl. Acad. Sci. USA*, **106**, 10171–10176.

77. Neville,M. and Rosbash,M. (1999) The NES-Crm1p export pathway is not a major mRNA export route in *Saccharomyces cerevisiae*. *EMBO J.*, **18**, 3746–3756.

78. Ho,J.H.-N., Kallstrom,G. and Johnson,A.W. (2000) Nmd3p is a Crm1p-dependent adapter protein for nuclear export of the large ribosomal subunit. *J. Cell. Biol.*, **151**, 1057–1066.

79. Lacombe,T., García-Gómez,J.J., de la Cruz,J., Roser,D., Hurt,E., Linder,P. and Kressler,D. (2009) Linear ubiquitin fusion to Rps31 and its subsequent cleavage are required for the efficient production and functional integrity of 40S ribosomal subunits. *Mol. Microbiol.*, **72**, 69–84.

80. Yu,L., Castillo,L.P., Mnaimneh,S., Hughes,T.R. and Brown,G.W. (2006) A survey of essential gene function in the yeast cell division cycle. *Mol. Biol. Cell*, **17**, 4736–4747.

81. Bernstein,K.A., Bleichert,F., Bean,J.M., Cross,F.R. and Baserga,S.J. (2007) Ribosome biogenesis is sensed at the start cell cycle checkpoint. *Mol. Biol. Cell*, **18**, 953–964.

82. Lee,J.C. and Henry,B. (1982) Binding of rat ribosomal proteins to yeast 5.8S ribosomal ribonucleic acid. *Nucleic Acids Res.*, **10**, 2199–2207.

83. Simoff,I., Moradi,H. and Nygard,O. (2009) Functional characterization of ribosomal protein L15 from *Saccharomyces cerevisiae*. *Current Genet.*, **55**, 111–125.

84. Rotenberg,M., Moritz,M. and Woolford,J.L. Jr (1988) Depletion of *Saccharomyces cerevisiae* ribosomal protein L16 causes a decrease in 60S ribosomal subunits and formation of half-mer polysomes. *Genes Dev.*, **2**, 160–172.

85. Lucioli,A., Presutti,C., Ciafre,S., Caffarelli,E., Fragapane,P. and Bozzoni,I. (1988) Gene dosage alteration of L2 ribosomal protein genes in *Saccharomyces cerevisiae*: effects on ribosome synthesis. *Mol. Cell. Biol.*, **8**, 4792–4798.

86. Gadal,O., Strauss,D., Braspenning,J., Hoepfner,D., Petfalski,E., Philippsen,P., Tollervey,D. and Hurt,E. (2001) A nuclear AAA-type ATPase (Rix7p) is required for biogenesis and nuclear export of 60S ribosomal subunits. *EMBO J.*, **20**, 3695–3704.

87. Chamberlain,J.R., Lee,Y., Lane,W.S. and Engelke,D.R. (1998) Purification and characterization of the nuclear RNase P holoenzyme complex reveals extensive subunit overlap with RNase MRP. *Genes Dev.*, **12**, 1678–1690.

88. Chu,S., Archer,R.H., Zengel,J.M. and Lindahl,L. (1994) The RNA of RNase MRP is required for normal processing of ribosomal RNA. *Proc. Natl Acad. Sci. USA*, **91**, 659–663.

89. Burger,F., Daugeron,M.-C. and Linder,P. (2000) Dbp10p, a putative RNA helicase from *Saccharomyces cerevisiae* required for ribosome biogenesis. *Nucleic Acids Res.*, **28**, 2315–2323.

90. Saveanu,C., Rousselle,J.C., Lenormand,P., Namane,A., Jacquier,A. and Fromont-Racine,M. (2007) The p21-activated protein kinase inhibitor Skb15 and its budding yeast homologue are 60S ribosome assembly factors. *Mol. Cell. Biol.*, **27**, 2897–2909.

91. Zanchin,N.I.T., Roberts,P., DeSilva,A., Sherman,F. and Goldfarb,D.S. (1997) *Saccharomyces cerevisiae* Nip7p is required for efficient 60S ribosome subunit biogenesis. *Mol. Cell. Biol.*, **17**, 5001–5015.

92. Hong,B., Brockenbrough,J.S., Wu,P. and Aris,J.P. (1997) Nop2p is required for pre-rRNA processing and 60S ribosome subunit synthesis in yeast. *Mol. Cell. Biol.*, **17**, 378–388.

93. Russell,I.D. and Tollervey,D. (1992) NOP3 is an essential yeast protein which is required for pre-rRNA processing. *J. Cell Biol.*, **119**, 737–747.

94. Kressler,D., Rojo,M., Linder,P. and de la Cruz,J. (1999) Spb1p is a putative methyltransferase required for 60S ribosomal subunit biogenesis in *Saccharomyces cerevisiae*. *Nucleic Acids Res.*, **27**, 4598–4608.

95. de la Cruz,J., Kressler,D., Rojo,M., Tollervey,D. and Linder,P. (1998) Spb4p, an essential putative RNA helicase, is required for a late step in the assembly of 60S ribosomal subunits in *Saccharomyces cerevisiae*. *RNA*, **4**, 1268–1281.

96. van Beekvelt,C.A., Kooi,E.A., de Graaff-Vincent,M., Riet,J., Venema,J. and Raué,H.A. (2000) Domain III of *Saccharomyces cerevisiae* 25 S ribosomal RNA: its role in binding of ribosomal protein L25 and 60S subunit formation. *J. Mol. Biol.*, **296**, 7–17.

97. Rutgers,C.A., Rientjes,J.M., van't Riet,J. and Raue,H.A. (1991) rRNA binding domain of yeast ribosomal protein L25. Identification of its borders and a key leucine residue. *J. Mol. Biol.*, **218**, 375–385.

98. Peculis,B.A. and Greer,C.L. (1998) The structure of the ITS2-proximal stem is required for pre-rRNA processing in yeast. *RNA*, **4**, 1610–1622.

99. Côté,C.A. and Peculius,B.A. (2001) Role of the ITS2-proximal stem and evidence for indirect recognition of processing sites in pre-rRNA processing in yeast. *Nucleic Acids Res.*, **29**, 2106–2116.

100. Pertschy,B., Schneider,C., Gnadig,M., Schafer,T., Tollervey,D. and Hurt,E. (2009) RNA helicase Prp43 and its co-factor Pfa1 promote 20S to 18S rRNA processing catalyzed by the endonuclease Nob1. *J. Biol. Chem.*, **284**, 35079–35091.

101. Jakovljevic,J., de Mayolo,P.A., Miles,T.D., Nguyen,T.M., Leger-Silvestre,I., Gas,N. and Woolford,J.L. Jr (2004) The carboxy-terminal extension of yeast ribosomal protein S14 is necessary for maturation of 43S preribosomes. *Mol. Cell*, **14**, 331–342.

102. Tabb-Massey,A., Caffrey,J.M., Logsden,P., Taylor,S., Trent,J.O. and Ellis,S.R. (2003) Ribosomal proteins Rps0 and Rps21 of *Saccharomyces cerevisiae* have overlapping functions in the maturation of the 3' end of 18S rRNA. *Nucleic Acids Res.*, **31**, 6798–6805.

103. Thomson,E. and Tollervey,D. (2005) Nop53p is required for late 60S ribosome subunit maturation and nuclear export in yeast. *RNA*, **11**, 1215–1224.

104. Gadal,O., Strauss,D., Petfalski,E., Gleizes,P.E., Gas,N., Tollervey,D. and Hurt,E. (2002) Rlp7p is associated with 60S preribosomes, restricted to the granular component of the nucleolus, and required for pre-rRNA processing. *J. Cell Biol.*, **157**, 941–951.

105. Hung,N.J., Lo,K.Y., Patel,S.S., Helmke,K. and Johnson,A.W. (2008) Arx1 is a nuclear export receptor for the 60S ribosomal subunit in yeast. *Mol. Biol. Cell*, **19**, 735–744.
106. Bradatsch,B., Katahira,J., Kowalinski,E., Bange,G., Yao,W., Sekimoto,T., Baumgartel,V., Boese,G., Bassler,J., Wild,K. *et al.* (2007) Arx1 functions as an unorthodox nuclear export receptor for the 60S preribosomal subunit. *Mol. Cell*, **27**, 767–779.
107. Hung,N.J. and Johnson,A.W. (2006) Nuclear recycling of the pre-60S ribosomal subunit-associated factor Arx1 depends on Rei1 in *Saccharomyces cerevisiae*. *Mol. Cell. Biol.*, **26**, 3718–3727.
108. Chen,I.J., Wang,I.A., Tai,L.R. and Lin,A. (2008) The role of expansion segment of human ribosomal protein L35 in nuclear entry, translation activity, and endoplasmic reticulum docking. *Biochem. Cell Biol.*, **86**, 271–277.
109. Pichon,J., Marvaldi,J. and Marchis-Mouren,G. (1975) The *in vivo* order of protein addition in the course of *Escherichia coli* 30 S and 50 S subunit biogenesis. *J. Mol. Biol.*, **96**, 125–137.
110. Nierhaus,K.H., Bordasch,K. and Homann,H.E. (1973) Ribosomal proteins. XLIII. In vivo assembly of Escherichia coli ribosomal proteins. *J. Mol. Biol.*, **74**, 587–597.
111. Jorgensen,P., Rupes,I., Sharom,J.R., Schneper,L., Broach,J.R. and Tyers,M. (2004) A dynamic transcriptional network communicates growth potential to ribosome synthesis and critical cell size. *Genes Dev.*, **18**, 2491–2505.